Studies of the Interaction of Excited Chloranil with Acrylonitrile, Methyl Methacrylate, and Styrene by Means of Laser Photolysis

Harumichi Kobashi, Hitoshi Gyoda, and Toshifumi Morita
Department of Chemistry, Faculty of Technology, Gunma University, Kiryu, Gunma 376

(Received February 5, 1977)

The behavior of electronically excited chloranil interacting with the titled vinyl compounds and solvents has been studied by means of the nanosecond laser photolysis technique. Semiquinone radicals and/or chloranil anions have been detected as transients except in the system containing styrene. Careful observation and analysis of the kinetic behavior of the transient absorptions reveal that these transients are brought about by the interaction of excited triplet state of chloranil with vinyl monomers and/or solvents. The logarithms of the quenching rate constants and rate constants of the formation of transients are linearly related to the ionization potentials of the vinyl monomers and solvents used. The mechanisms of the triplet quenching and transient formation can reasonably be interpreted by taking the relaxed triplet-state complex with a charge-transfer character into account as the precursor leading to the production of semiquinone radicals, chloranil anions, and other intermediate compounds.

Several investigations of the behavior of the chloranil (CA) molecule, as a representative quinone, have been performed with reference to electron donor–acceptor (EDA) complex formations,[1)] photochemical reactions,[2)] electronic states,[3)] and electrical conductivities.[4)] Among these, the photopolymerization mechanism in which the excited state of CA plays an important role is one of the most interesting. Mikawa and his co-workers[5,6)] have reported, in their studies concerning the photosensitized polymerization mechanism of *N*-vinylcarbazole (VCZ) by CA, that electron transfer occurs from VCZ to excited CA, producing the CA anion (CA^-) and the VCZ cation, and that VCZ cations behave differently depending as the polarity of the solvents used; in a polar solvent such as acetone cyclodimerization occurs,[5,6)] but in a nonpolar solvent such as benzene catonic polymerization occurs without any induction period.[6)] In contrast to their studies, we have confirmed[7)] that acrylonitrile (AN), methyl methacrylate (MMA), and styrene (ST) react with excited CA and that radical polymerization occurs after a well-defined induction period, during which addition compounds between CA and the vinyl monomers used are produced both in polar and in nonpolar solvents. The difference in the polymerization mechanisms between the two series of systems mentioned above seems to be originally attributable to a difference in the ionization potentials of the vinyl monomers. Mikawa and his co-workers used vinyl monomers with relatively small ionization potential values, while we used vinyl monomers with relatively large ionization potentials. It is well known that, because of their strong electron-accepting and hydrogen-abstracting properties, CA molecules in the excited states interact with various electron and/or hydrogen donors, even with some solvents as well, to produce semiquinone anions and/or radicals.[9–14)] Furthermore, the presence of the excited triplet state EDA complex has been suggested by Tsubomura and his co-workers,[10)] who used a microsecond flach-photolysis technique in a fluid solution of CA–benzene and CA–acetone systems.

Since the excited CA behaves, as has been mentioned above, in very different ways as systems studied vary, very careful experiments should be performed to determine the photosensitized polymerization mechanisms, with special attention paid to the interaction between the excited CA and the vinyl monomers in both the presence and absence of solvents.

In this work, as a part of our studies of the polymerization mechanisms photosensitized by CA, nanosecond ruby laser photolysis has been carried out, with special attention paid to the detection of transients, tracing their origins, and making sure of the kinetic behavior of the transients produced by the interactions between excited CA and AN, MMA, ST, and tetrachlorohydroquinone in the presence and absence of dichloroethane, trichlorotrifluoroethane, and acetonitrile as solvents. The interactions of excited CA with dichloroethane, trichlorotrifluoroethane, and acetonitrile have also been studied in order to obtain further knowledge.

Experimental

Apparatus and Measurements. The nanosecond laser photolysis apparatus used in the present study is shown schematically in Fig. 1. A giant pulse of 694 nm, with an output of *ca.* 2 J, was generated with a ruby laser (JEOL, JLS-R3A) Q-switched by a rotating prism and passed through an ADP frequency doubler to obtain a second harmonic for excitation. After the elimination of an undoubled fundamental pulse with a 10-mm cell containing a saturated cupric sulfate solution, the doubled laser pulse of a 23 ns half-duration, with a wavelength of 347 nm, was supplied into a sample in a 10-mm quartz cell mounted on a cell holder. The output energy of this laser pulse was measured with a thermopile (TRG, Model 107) combined with a recorder (Hitachi, Model 056) through a microvolt meter (Ohkura Electric Co., AM-1001). The power of the pulse through the sample cell was also measured with the same thermopile each time photolysis was done. In each measurement, the spectra of the transients were easily corrected to the same laser intensity by this way after confirmation of the absorption arising through the one-photon process. Since the laser intensity effect on the absorption intensities of transients should be checked beforehand, a small part of the exciting pulse, which was reflected with a beam splitter placed between the solution filter and the sample cell, was simultaneously monitored by means of a photomultiplier, PM-1 (HTV, 1P28) with a high response. Glass plates were employed to reduce the intensity of the exciting pulse. A xenon flash of *ca.* 600 μs half-width from a stroboscope (SUNPACK, Model 107) was used as an analysis flash for the detection of the transients; its peak

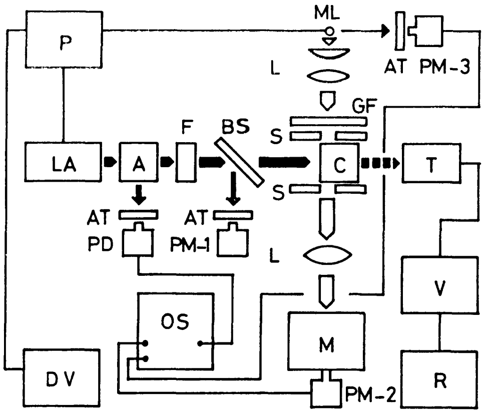

Fig. 1. Schematic diagram of the apparatus for nanosecond laser photolysis. LA: ruby laser, P: power supply and timing circuit, DV: degital voltmeter (Hitachi, Type 028-0010) by which supplied voltage to a pumping flash is externally read out. A: ADP frequency doubler, F: $CuSO_4$ aq filter, BS: beam splitter which is removed in ordinary experiments, C: sample cell, T: thermopile, V: μV meter, R: recorder, ML: monitor flash lamp, L: lens, GF: glass filter, S: variable slit, M: monochromater, PM-1, 2, and 3: photomultipliers, PD: photodiode, AT: light attenuator, OS: oscilloscope.

was synchronized electronically with the laser pulse. After crossing through the sample cell at right angles with respect to the laser beam, this analyzing light was collected by a lens and focussed onto the slit of a grating monochromator which was a part of a Hitachi UV-VIS spectrophotometer (model 139). An appropriate combination of glass filters at the front of the cell was used not only to remove the second-order stray light, but also to prevent the sample solution from being illuminated undesirably. The exit light from the monochromator was received by a photomultiplier tube, PM-2 (HTV, R446), loaded with a 75Ω resistor. The output signal from this tube was displayed on a 200 MHz oscilloscope (Iwatsu, SS-6200) which was triggered externally by the pulse from a photodiode (EG & G, SGD-100A) monitoring the laser pulse scattered from the ADP crystal. The rise and decay profile of a single sweep of the signal was photographed on X-ray films. Further, a third photomultiplier tube, PM-3 (HTV, 1P28), was used to correct the intensity fluctuation of the analysis lamp. The response of the photomultiplier which was exposed to the analyzing flash, attenuated by half-transparent papers, was guided into the second channel of the oscilloscope; thus, a reference signal to the signal corresponding to a 100% transmittance of the analyzing light was obtained. Operation using the chopped-sweep function of the oscilloscope made it possible to photograph this reference signal and the decay of the transient absorption simultaneously. Then decay patterns of the long-life transients could be analyzed accurately, even in a time region where the intensity of the analyzing flash was no longer 'steady.' In addition, air conditioning was needed to obtain a constant output of second harmonics, because the best matched axis of the ADP crystal to the fundamental laser beam was quite sensitive to room temperature. The variation in the temperature in an operating room was controlled in the range of ±1.0 °C during laser photolysis. Thus, the nanosecond time resolution was obtained by the use of this instrumental system and the transient spectra, and the rise and/or decay curves could be followed up quantitatively over the time range from the starting time of laser oscillation to *ca.* 200 μs.

When samples were photolyzed at the temperature of liquid nitrogen, the cell holder was replaced by a quartz vessel with three flat windows at right angles with each other. In the present study, all the experiments, except for the system of CA and MMA in EPA (ethylether : isopentane : ethanol=5 : 5 : 2 in volume), were carried out at room temperature.

The EDA complex formation in the ground state between CA and the vinyl compounds was examined by measurements of the absorption spectra using Hitachi 124 and 139 spectrophotometers. To describe the results briefly in this section, spectroscopic evidence for complexing in 1,2-dichloroethane was not observed in the CA–AN system. On the other hand, in the CA–MMA system a new broad band appeared around 315 nm as a shoulder of the falling branch of the intense π-π^* transition of uncomplexed CA, which has a maximum at 292 nm, and in the CA–ST system a band having its maximum at 420 nm was remarkably observed. Both of the latter bands can be reasonably interpreted as charge-transfer (CT) bands by the aid of the Benesi-Hildebrand equation, the Ketelaar equation, and the linear relation of CT-band energies against the ionization potentials of the donors.

Materials. The chloranil (Tokyo Kasei, G. R. grade) was purified by a recommended method,[15] *i.e.*, recrystallized twice from benzene and chromatographed on freshly baked calcium carbonate, using purified benzene as the eluant in order to eliminate any acidic impurities. After one more recrystallization, a vacuum sublimation was undertaken just before use. The acrylonitrile (Wako, G. R. grade) was washed with 5% NaOHaq, phosphoric acid, and distilled water, three times each. After drying over potassium carbonate, it was fractionally distilled twice in an atmosphere of nitrogen under reduced pressure. Methyl methacrylate (Wako, G. R. grade) was purified by the method described elsewhere.[16a] The styrene (Wako, Practical grade) was treated with 5% NaOHaq, washed with distilled water, dried over calcium chloride and barium oxide, and purified twice by fractional distillation in a nitrogen atmosphere under reduced pressure. These vinyl monomers were passed through a short column of molecular sieves *(Zeolite)* and silica gel immediately before use. The tetrachlorohydroquinone (CA-H_2) (Tokyo Kasei, C. P. grade) was purified as follows. The faint pink substance which was obtained by two recrystallizations from glacial acetic acid and successive washing with hot water was treated with an aqueous solution of sodium sulfite in order to reduce, chemically, a little amount of contaminated CA to the corresponding hydroquinone. The precipitates which were obtained by adding an adequate amount of hydrochloric acid to the aqueous solution were washed throughly with ethanolic water and dried. The raw product was sublimed under a vacuum. A pure white material was thus obtained; it was found by usual analytic methods, to be tetrachlorohydroquinone. The benzophenone, which was used as a standard to estimate the extinction coefficient of the triplet chloranil, CA(T), was purified by the method described elsewhere.[16b] The 1,2-dichloroethane (DCE), acetonitrile, trichlorotrifluoroethane, ethyl ether, and isopentane used as solvents were purified by ordinary methods,[17] while the ethanol (Kanto Chemical Co., G. R. grade) was used without further purification. The solutions subject to laser photolysis were deaerated carefully by the freeze-pump-thaw cycle method. The concentration of CA in the solution was controlled in the range of $(1\text{—}3)\times10^{-3}$ mol dm^{-3}.

Results and Discussion

Identification of Transients. CA–DCE System:

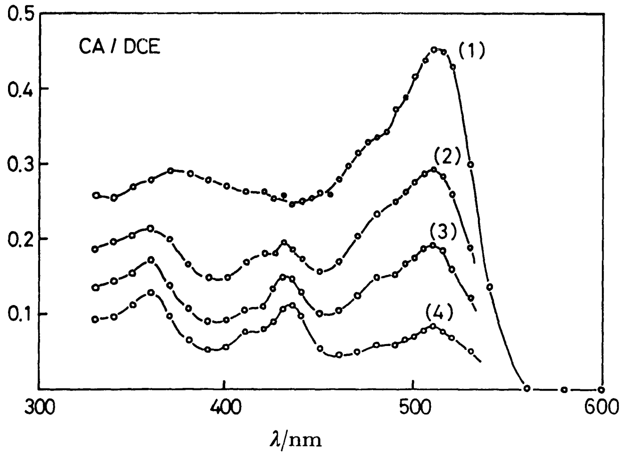

Fig. 2. Time resolved transient spectra for CA–DCE system: $[\mathrm{CA}]=2\times10^{-3}\ \mathrm{mol\ dm^{-3}}$. The delay time from the laser pulsing, (1) 0, (2) 2, (3) 4, (4) 8 μs.

Figure 2 shows the time-resolved spectra after laser excitation for the system of CA alone in DCE. Observed bands with maxima at 510 and 370 nm in the spectrum immediately after pulsing closely resemble those of CA(T) in several solvents illustrated in Fig. 1 of Ref. 10 and discussed in Ref. 9. From an examination of the exponential decay of the 510 nm band, its lifetime was determined to be 5.6 μs in the deaerated solution and 0.45 μs in the aerated solution. These values are nearly equal to those for other solvent systems previously reported.[9a,9c] This is other evidence that this band belongs to CA(T). According to the investigation by the authors of Ref. 10, the 370 nm band is also attributable to CA(T). From the standpoint of these authors, we may also regard this band as belonging to CA(T), although, in our case, the band around 370 nm behaves, after a lapse of time, in the somewhat complicated manner to be described below. With the lapse of time, the spectrum is gradually replaced by another with band maxima at 430 and 360 nm. As regards these two bands, we obtained the following information: (a) Both of these bands had a relatively long life, and they decayed with similar time profiles. (b) Both the shape of the 430 nm band and the position of the 360 nm band closely resemble those studied in Ref. 10, which were attributed to semiquinone radicals. (c) Our experiments, performed by replacing the DCE by trichlorotrifluoroethane (with no hydrogen atom), revealed the non-existence of these bands. Using the microsecond-flash-photolysis technique, in which the irradiation of light over a broader range of wavelengths than in the case of nanosecond-laser photolysis is not avoided, Tsubomura and his co-workers[10] have reported the appearance of the bands attributable to the semiquinone radicals produced by the chlorine atom transfer to CA-(T) from the Diflon S3 used as a solvent. This seems to indicate that the quite high excess vibrational energy in the lowest excited electronic state might be required for the abstraction of a 'heavy' chlorine atom in this system. An inspection of this information allows us to consider these two bands as belonging to semiquinone radicals of CA, CAH·, which have been produced by hydrogen-atom abstraction from the solvent.

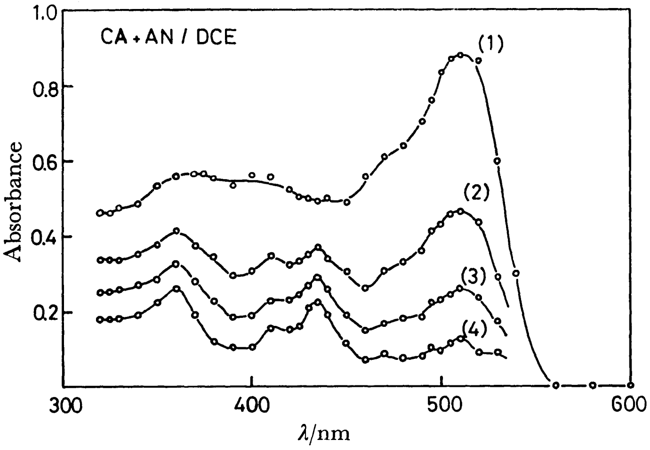

Fig. 3. Time resolved transient spectra for CA–AN–DCE system: $[\mathrm{CA}]=2\times10^{-3}\ \mathrm{mol\ dm^{-3}}$, $[\mathrm{AN}]=0.76\ \mathrm{mol\ dm^{-3}}$. The delay time from the laser pulsing, (1) 0, (2) 2, (3) 4, (4) 8 μs.

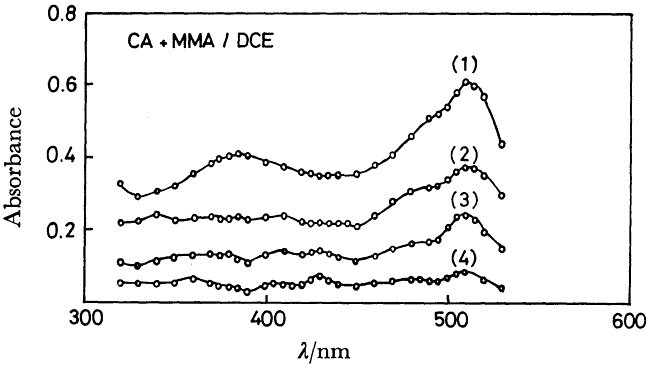

Fig. 4. Time resolved transient spectra for CA–MMA–DCE system: $[\mathrm{CA}]=2\times10^{-3}\ \mathrm{mol\ dm^{-3}}$, $[\mathrm{MMA}]=0.94\ \mathrm{mol\ dm^{-3}}$. The delay time from the laser pulsing, (1) 0, (2) 0.1, (3) 0.2, (4) 0.4 μs.

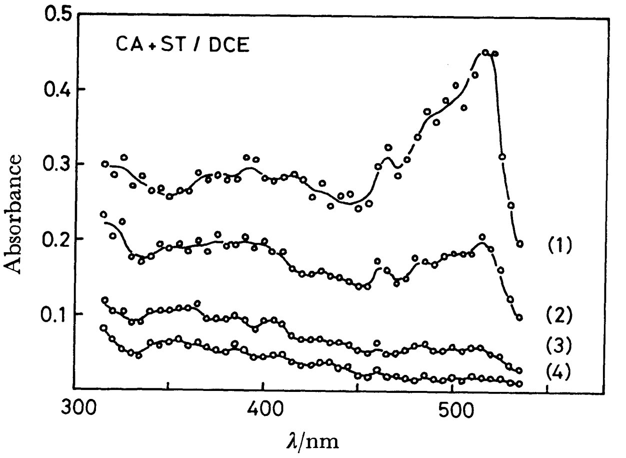

Fig. 5. Time resolved transient spectra for CA–ST–DCE system: $[\mathrm{CA}]=1.7\times10^{-3}\ \mathrm{mol\ dm^{-3}}$, $[\mathrm{ST}]=0.87\times10^{-3}\ \mathrm{mol\ dm^{-3}}$. The delay time from the laser pulsing, (1) 0, (2) 0.2, (3) 0.7, (4) 1.5 μs.

CA–Vinyl Monomer–DCE Systems: The transient absorption spectra changing with the lapse of time are exemplified for several systems in Fig. 3 (CA–AN–DCE), Fig. 4 (CA–MMA–DCE) and Fig. 5 (CA–ST–DCE).

The spectral features of the CA–AN–DCE system closely resemble those of the CA–DCE system (Figs. 2 and 3). In the CA–MMA–DCE system containing a high concentration of MMA the 510 nm absorption of CA(T) decays rapidly and scarcely no spectral components of CAH· remain (Fig. 4). In the CA–ST–DCE system containing a high concentration of ST (≥ 0.1 mol dm^{-3}), no transient could be observed at all. However, in the same system containing a low concentration of ST, where ground-state EDA-complex formation is negligible, the initial spectrum rapidly disappears, keeping its spectral aspects without any bands attributable to semiquinone radicals being distinguishable (Fig. 5).

Kinetic Behavior of the 425 nm Band. The behavior of the absorption band monitored at 425 nm in the CA–DCE and CA–AN–DCE systems was followed from the time just after pulsing to *ca.* 10 μs (Fig. 7a). The decay of this absorption apparently obeyed the second-order kinetics after a rapid rise just after pulsing. The absorption intensity at the pulse end was recognized to be linearly related with the power of the laser for excitation. This means that this band arose through a one-photon process. It was observed that the 510 nm band also arose through a one-photon process. Since species bearing the 425 nm absorption in our systems are CA(T) and CAH·, it is important to check if CAH· comes from the singlet excited state of CA, CA(S) or from CA(T). This problem can be clarified by observing and analyzing the addition effect of ST, CAH$_2$, and MMA, as will be described below.

(a) As has previously been suggested for the CA–ST–DCE system, CA(T) is quenched rapidly, keeping its spectral features, and no observable transient like CAH· exists during the quanching process. This indicates that the initial appearance of the 425 nm band is due to CA(T). We will further discuss what would happen if CAH· is assumed to be produced in CA(S). The disappearance of CAH· might occur following self-disproportionation:[11a)]

$$\text{CAH}\cdot + \text{CAH}\cdot \longrightarrow \text{CA} + \text{CAH}_2 \qquad k_\text{d}, \qquad (1)$$

and/or the conventional mechanism[19)] described below, which is generally accepted for a radical polymerization with an induction period:

$$\text{CAH}\cdot\ (\text{or} \sim\!\text{CA}\cdot) + \text{ST} \longrightarrow \sim\!\text{ST}\cdot \qquad k_\text{o}, \qquad (2)$$

$$\sim\!\text{ST}\cdot + \text{CA} \longrightarrow \sim\!\text{CA}\cdot \qquad k_\text{z}, \qquad (3)$$

$$\sim\!\text{ST}\cdot + \text{ST} \longrightarrow \sim\!\text{ST}\cdot \qquad k_\text{p}. \qquad (4)$$

Here, k_d, k_o, k_z, and k_p are the rate constants of Reactions 1, 2, 3, and 4 respectively, and $k_\text{d}=1.4\times10^9$ mol^{-1} dm^3 s^{-1} (to be described in detail later), $k_\text{p}=123$ mol^{-1} dm^3 s^{-1},[18)] $k_\text{z}/k_\text{p}=2040$ at 50 °C,[18)] and $k_\text{o}<k_\text{p}$.[19)] An inspection of the values of those rate constants and the relation between them indicates that the disappearance of CAH· would be efficiently subject to self-disproportionation, which, in turn, is very slow compared to the disappearance of CA(T) under our experimental conditions. On the assumption that CAH· would be produced from CA(S), therefore, the 425 nm band due to CAH· should remain during the spectral change in question. This contradicts the experiments and suggests that CAH· is not produced from CA(S).

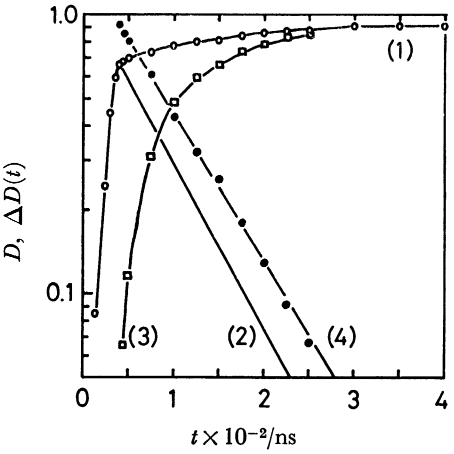

Fig. 6. Graphical analysis of the decay function of transient observed at 425 nm in CA–CAH$_2$–DCE system: [CA]$=2.36\times10^{-3}$ mol dm^{-3}, [CAH$_2$]$=2.58\times10^{-3}$ mol dm^{-3}. Curve (1): observed, (2) triplet decay, (3): CAH· rise, $D(t)=(1)-(2)$, (4): rate determining curve for CAH· formation, $\Delta D(t)=D_\text{p}-D(t)$; $D_\text{p}=0.92$.

(b) In order to clarify more distinctly the kinetic behavior of the absorption at 425 nm, we examined the addition effect of CAH$_2$ to the CA–DCE system. The decay profile followed up at 425 nm was analyzed kinetically for this system containing a small amount of CAH$_2$ (2.6×10^{-3} mol dm^{-3}), where no spectroscopic evidence exists as to a ground-state complex formation between CA and CAH$_2$. The analyzed results regarding the kinetic behavior of the 425 nm absorption can be reasonably explained by considering that the CA(T) which is generated at first will be quenched dynamically by CAH$_2$ and that the CAH· will increase through the CA(T)+CAH$_2$→2CAH· reaction. In fact, in our experiments, the increase in the 425 nm band was shown directly on the oscilloscope. Furthermore, this band was distinctly confirmed to belong to CAH· by an examination of its position and band shape as distinguished from all others in the spectrum. Figure 6 shows the results analyzed carefully. When the contribution of CA(T) to the absorbance at this wavelength, (2), is subtracted from the observed signal, (1), Curve (3) results; this curve refers to the growth of CAH· itself. Since the decay rate of the radical is much lower than that of the triplet (its decay time, $\tau_\text{T}=73$ ns in the present system), the disappearance of the former can reasonably be neglected during such a short time interval as in our experiments. Then, the subtraction of Curve (3), $D(t)$, from the peak value, D_p, of the observed curve gives Curve (4), $\Delta D(t)$, from which the time constant of CAH· formation can be obtained. By these procedures, it was quantitatively ascertained that the initial absorption at 425 nm was certainly due to CA(T) and that the rise time of CAH· ($\tau_\text{r}=83$ ns) was equal to the decay time of CA(T), within our limits of experimental accuracy. That is to say, CAH· is certainly produced *via* CA(T). Another support to this reasoning is also obtained from a comparison of the decay patterns of the 425 nm absorption between the CA–DCE and CA–CAH$_2$–DEC systems. Figure 7

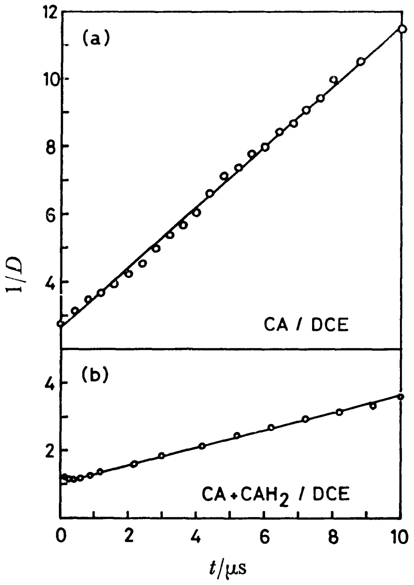

Fig. 7. Plots of second-order kinetics for the decay observed at 425 nm. a: CA–DCE, b: CA–CAH_2–DCE system.

shows the curves obtained by plotting the reciprocal of the optical density (D) against the lapse of time for these two systems. In the CA–CAH_2–DCE system (Fig. 7b), after the complete disappearance of CA(T) and the complete rising of CAH· at the initial stage of time lapse, the decay of the 425 nm band with reference to CAH· proceeds along a good straight line (Line b). In the CA–DCE system, there is apparently a straight line (Line a) following the second-order kinetics (Fig. 7a). If the transients were the same for both systems, their decay constants and, accordingly, the slopes of Line a and Line b would have to be identical. However there is a remarkable discrepancy between these two slopes, as may be seen in Fig. 7. Since Line b is the very realization of the kinetic behavior of CAH·, Line a does not embody the kinetic behavior of only CAH·. Moreover, a close inspection of Fig. 7a shows the string of circles to form a slightly S-shaped curve. We observed, further, a little more striking S-shaped curve for this system when the kinetic behavior was followed at 430 nm. This decay picture is characteristic when the absorption of a long-life transient, obeying the second-order decay kinetics, overlaps that of another transient decaying exponentially. Therefore, the observations can be understood by reasoning that, because of the superpostion of the CAH· rise and decay on the CA(T) decay, the absorption at 425 nm in the CA–DCE system apparently behaves as if the initially formed CAH· has decayed alone and smoothly with the second-order kinetics. As has been mentioned in the previous section, the 425 nm band in the CA–AN–DCE system also decayed apparently following the second-order kinetics from the time immediately after pulsing. This feature is the reflex of the same situation as that of Fig. 7a. These interpretations well correspond to those of Kemp and Porter[9b] as to the origin of the durosemiquinone radical produced by microsecond-flash photolysis in liquid paraffin.[20] Now, we can estimate the decay constant of CAH· accurately from Fig. 7b. From the slope of Line b, which strictly obeys the second-order kinetics, the decay constant was determined to be $2.8\times10^5\varepsilon l$ mol^{-1} dm^3 s^{-1}, where ε is the molar extinction coefficient of CAH· at 425 nm and where l is the width of the photolyzed part, which was estimated as 0.70 cm from the size of the second harmonics for excitation. The estimated value, 1.4×10^9 mol^{-1} dm^3 s^{-1}, was obtained using the reference value of ε, 7.3×10^3 mol^{-1} dm^3 cm^{-1}.[11a)]

(c) In the system containing a high concentration of MMA, the absorption at 425 nm due to CA(T) early disappears exponentially, and after this rapid decay the remaining transient, CAH·, gradually decays with a long life. Although no exact analysis on the growth of CAH· was done in the DCE solvent, the above behavior and the results of kinetic analysis for CA^- and CAH· in the CA–MMA–CH_3CN system described in the next section may allows us to consider that the formation of CAH· arises from CA(T). It is noteworthy that CAH· is surely generated in this system, also through interaction between CA(T) and MMA.

Therefore, from the above discussions it can safely be concluded that the origin of CAH· in the CA–DCE system, regardless of the presence or absence of the additives (ST, CAH_2, AN, and MMA), is the triplet state of CA.

Production of the Chloranil Anion in the Polar Solvent. The time-resolved spectra obtained by the laser photolysis for the CA–CH_3CN system are shown in Fig. 8a. CA(T), with maxima at 510 and 370 nm, decays relatively fast, and the absorption bands of maxima at 450, 430, and 360 nm become conspicuous 5 μs after flashing. These aspects closely resemble those obtained by the microsecond-flash photolysis for the same system.[10] It has already been known that CA^- has absorption bands at 448, 422, and 321 nm.[23] From this knowledge and from a comparison with the results for the CA–DCE system (Fig. 2), it is possible to deduce that, among the bands observed, the 450 nm band is brought about mainly from CA^-, the 360 nm band mainly from CAH·, and the 430 nm band from both CA^- and CAH·. On adding ST to this solution, CA(T) decayed rapidly, keeping its original aspects and without producing any transients, in the same way as in the case of the DCE solution. On the other hand, however, as may be seen in Fig. 8b, the addition of 1.0 mol dm^{-3} MMA to the solution causes a rapid decrease in CA(T) and does not prevent CA^- and CAH· from being produced and living for a relatively long time. The kinetic behavior of the band with its maximum at 450 nm was analyzed carefully in the same manner as in the CA–CAH_2–DCE system. The results revealed that CA^- grow simultaneously with the decay of CA(T). The kinetic analysis at 420 nm also led to the same result. Therefore, which one of the two species, CA^- or CAH·, is the primary transient is not proven, but it is elucidated that both of them come from CA(T).

Some observations have now established that the weak EDA complex in a polar solvent is photolyzed to produce the anion of an electron acceptor due to ionic dissociation in the first excited singlet state.[21] However, for the CA–MMA complex in acetonitrile, no

TABLE 1. QUENCHING RATE CONSTANTS FOR TRIPLET CHLORANIL BY VINYL MONOMERS AND THEIR IONIZATION POTENTIALS (I)

Quencher	I/eV	Solvent	k_q/mol^{-1} dm^3 s^{-1}
AN	10.91	DCE	3.1×10^4
MMA	9.8	DCE	5.1×10^6
		CH_3CN	6.7×10^6
ST	8.47	DCE	2.5×10^9
		CH_3CN	8.0×10^9

indication of the direct production of the anion *via* the excited singlet state has been obtained. This may be interpreted as follows. As the CT band maximum of the CA–MMA complex is located at a higher energy than its locally excited band within the CA molecule, the lowest excited singlet state of the complex is probably similar in nature to that of uncomplexed CA. Accordingly, a rapid intersystem crossing in the complex may occur, as in CA, immediately after pumping to the singlet state, this crossing being then followed by ionic dissociation.

The Mechanism of Triplet Quenching and Semiquinone Formation. As is illustrated in Figs. 3, 4, and 5, CA(T) is quenched by each of the vinyl monomers. The rate of decay at 510 nm obeyed a Stern-Volmer-type relation in the relatively low concentration range of quenchers: $1/\tau=1/\tau_0+k_q[Q]$, where τ and τ_0 are the decay times of CA(T) in the presence and absence of a quencher, Q, respectively, where [Q] is the concentration of Q, and where k_q is the quenching rate constant. The values of the rate constants are listed in Table 1. The values of k_q increase with a decrease in the ionization potentials of the quenchers, and an increase in the solvent polarity tends to enhance the quenching by vinyl monomers, especially by ST. This means that the CT interaction between CA(T) and ST is quite responsible for the quenching.

For the purpose of estimating the quantum yields of the transients, we estimated the molar extinction coefficient of CA(T) at 510 nm by comparison with that of the benzophenone triplet at 532.5 nm in benzene,[22] assuming the triplet yield of CA to be unity. The estimated value was $(7.2\pm1.3)\times10^3$ mol^{-1} dm^3 cm^{-1} in DCE, nearly equal to that of duroquinone triplet in cyclohexane or benzene.[22] Using this value and that of CAH·[11] or CA^-,[23] the yield, ϕ, of the CAH· or CA^- formed from CA(T) can be approximately evaluated from the time-resolved spectra for the systems shown in Figs. 2, 3, 4, and 8 and for the system of CA in neat AN or MMA as well. In this estimation, the triplet yield of CA has already been assumed to be unity, and it was assumed that there was no effect of the solvent change upon the absorptivity of CA(T). Since the observed ϕ value corresponds approximately to $k_{ri}[M_i]\tau$, where k_{ri} is the second-order rate constant for the transient arising from the interactions between CA(T) and the reactant, M_i (the vinyl compound and/or solvent), where $[M_i]$ is the concentration of M_i, and where τ is the lifetime of CA(T) under the examining conditions, one can estimate k_r easily. These results are summarized in Table 2, along with the corresponding ϕ values. The low yields of CAH· and CA^- imply that other quenching processes are efficiently competing with their formation. One of the competing processes is the rather efficient production of an intermediate compound during the induction period of the ST or MMA polymerization photosensitized by CA.[7] That is to say, the quenching of CA(T) by vinyl monomers results mainly in the production of adducts between CA and monomers, and partly in the formation of CAH· and/or CA^-.

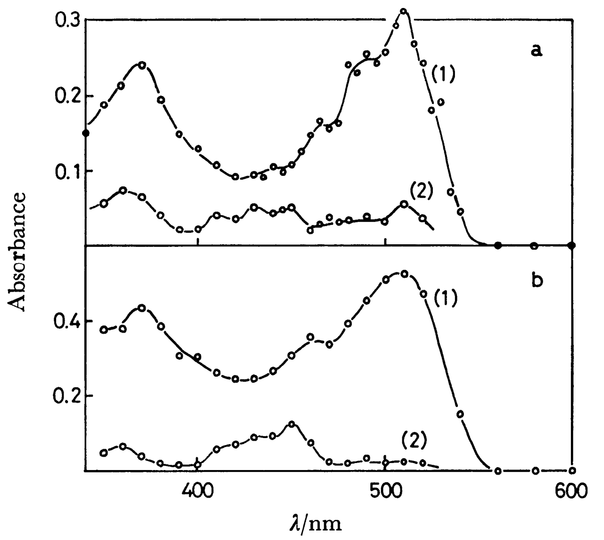

Fig. 8. Transient absorption spectra obtained by nanosecond laser photolysis for CA–CH_3CN and CA–MMA–CH_3CN systems. a: $[CA]=1.5\times10^{-3}$ mol dm^{-3}, b: $[CA]=3\times10^{-3}$ mol dm^{-3}, $[MMA]=1.0\times10^{-3}$ mol dm^{-3} in acetonitrile.

TABLE 2. YIELD OF CAH· AND CA^- FOR SEVERAL SYSTEMS AND RATE CONSTANTS FOR THEIR FORMATION

Transient	System	ϕ	k_r/mol^{-1} dm^3 s^{-1}
CAH·[a)]	CA-DCE	0.19	3×10^3
	CA-AN	0.20	7×10^3
	CA-MMA	0.08	4×10^5
CA^- [b)]	CA-CH_3CN	0.08	9×10^2
	CA-MMA-CH_3CN	0.15	9×10^5

a) The molar extinction coefficients at 435 and 420 nm in dioxane[11] were used for all our systems: $\varepsilon(435)=7.7\times10^3$ mol^{-1} dm^3 cm^{-1}, $\varepsilon(425)=7.3\times10^3$ mol^{-1} dm^3 cm^{-1}. b) $\varepsilon(450)=9.7\times10^3$ mol^{-1} dm^3 cm^{-1} [23] was used.

When the logarithms of the formation-rate constants (k_r) of CAH· are plotted against the ionization potentials of the reactants, a linear relationship is obtained. Plots of log k_q against the ionization potentials of the quenchers also show a linearity (Fig. 9). An inspection of these results reveals that the hydrogen transfer as well as the triplet quenching may be swayed by the CT interaction.[25] Accordingly, the existence of a triplet state complex as a precursor may be safely assumed, from which the electron transfer, the hydrogen transfer, the formation of intermediate componds for polymerization, and a return to the ground state may be thought to take place. In this connection, the next

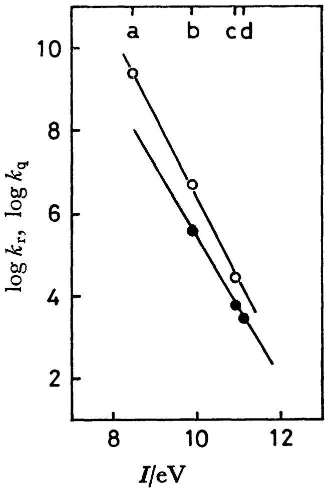

Fig. 9. Plots of log k_r and log k_q, respectively, against ionization potentials (I). The horizontal scale a, b, c, and d refer to I values of ST, MMA, AN, and DCE, respectively.
●: log k_r, ○: log k_q.

observation seems to supply additional support for the CT character of the triplet intermediate. The photolysis for the CA–MMA complex at 77 K in EPA, where the ground-state conformation of the complex may be almost frozen, gave a new, weak, transient absorption in the 550—650 nm region like that of the triplet EDA complex between CA(T) and benzene or between CA(T) and acetone,[10] although at room temperature such a broad band was not found, not even in a more concentrated MMA solution. These aspects are shown in Fig. 10. As the ionization potential of MMA is not very different from that of acetone, it may be possible to regard that absorption as the band arising from the CT interaction between CA(T) and MMA.

The observations and considerations described above allow us to explain the interaction mechanisms of the excited state of CA with the vinyl monomers used in the present work by assuming the following scheme:

$$\begin{tikzcd}
\mathrm{CA(T)} + \mathrm{M} \arrow[r] & \underset{(\mathrm{TC})}{{}^3(\mathrm{CA}^{\delta-}\cdots\mathrm{M}^{\delta+})} \arrow[r] \arrow[dl] \arrow[dr] & \mathrm{CAH}\cdot + \mathrm{M}'\cdot \\
\mathrm{CA(S_0)} + \mathrm{M} & & \mathrm{P} \qquad \text{and/or} \quad \mathrm{CA}^- + \mathrm{M}^+
\end{tikzcd}$$

where M means the vinyl monomer; TC, the triplet complex, and P, the intermediate compound which relates to polymerization. The main features of this scheme resemble that proposed for the photoreduction of benzophenone by amines.[25,26] Whether the semiquinones appear or not may be determined by the relative efficiency of each process under the effect of surrounding solvent molecules upon the triplet-state complex. In so far as our present systems are concerned, both electron transfer and hydrogen abstraction by CA(T) should take place from a relaxed equilibrium state of the triplet intermediate after solvent reorientation is realized, because the triplet quenching is rather slow compared to the diffusion-controlled rate.

This conclusion is very interesting compared to the assumption[26] of the existence of a non-relaxed triplet-state encounter complex from which hydrogen-atom abstraction occurs, competing with the ionic dissociation, for the benzophenone-tertiary amine systems with relatively low ionization potentials.

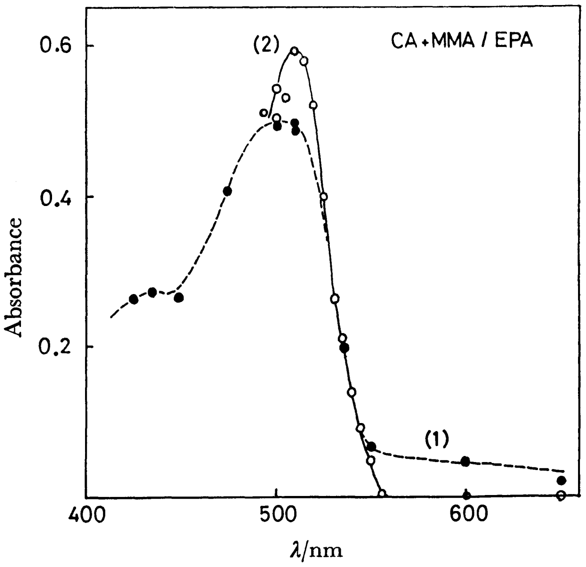

Fig. 10. Transient absorption spectra immediately after pulsing for CA–MMA–EPA and CA–MMA–DCE systems. (1): CA–MMA–EPA system at 77 K, [MMA]=0.48 mol dm^{-3}, (2): CA–MMA–DCE system at room temperature, [MMA]=0.94 mol dm^{-3}.

The authors wish to thank Mr. Norihito Suzuki and Mr. Kazuo Maeda for their experimental assistance. One of the authors (H. K.) would like to acknowledge the award of a Grant-in-Aid for Scientific Research from the Ministry of Education.

References

1) a) G. Briegleb, "Electronen-Donator-Acceptor-Komplexe," Springer-Verlag, Berlin (1962); b) R. Foster, "Organic Charge-Transfer Complexes," Academic Press, London (1969); c) R. S. Mulliken and W. B. Person, "Molecular Complexes," Wiley-Interscience, New York (1969).

2) a) G. O. Schenck, *Z. Electrochem.*, **64**, 997 (1960); b) D. Bryce-Smith and A. Gilbert, *Tetrahedron Lett.*, **1964**, 3471; c) J. A. Barltrop and B. Hesp, *J. Chem. Soc. C*, **1967**, 1625; d) T. Nogami, K. Yoshihara, H. Hosoya, and S. Nagakura, *J. Phys. Chem.*, **73**, 2670 (1969); T. Nogami, K. Yoshihara, and S. Nagakura, *Bull. Chem. Soc. Jpn.*, **45**, 122 (1972); T. Yamaoka and S. Nagakura, *ibid.*, **44**, 2971 (1971); e) R. Foster, *J. Chem. Soc., Perkin Trans. 1*, **1974**, 1318.

3) a) G. Giacometti, P. L. Nordio, and G. Rigatti, *Nuovo Cimento*, **23**, 433 (1962); b) A. Bieber and J. J. Andre, *Chem. Phys.*, **5**, 166 (1974); c) M. Sebti, F. Dupuy, J. Mégel, and G. Nouchi, *C. R. Acad. Sci., Ser. B*, **272**, 123 (1971); d) H. P. Trommsdorff, P. Sahy, and J. Kahane-Paillous, *Spectrochim. Acta, Part A*, **26**, 1135 (1970); H. P. Trommsdorff, *J. Chem. Phys.*, **56**, 5358 (1972); e) E. A. Braude, *J. Chem. Soc.*, **1945**, 490.

4) D. D. Eley, H. Inokuchi, and M. R. Willis, *Discuss. Faraday Soc.*, **28**, 54 (1959).

5) Y. Shirota, K. Kawai, N. Yamamoto, K. Tada, T. Shida, H. Mikawa, and H. Tsubomura, *Bull. Chem. Soc. Jpn.*,

45, 2683 (1972).

6) K. Tada, Y. Shirota, S. Kusabayashi, and H. Mikawa, *Chem. Commun.*, **1971**, 1169; K. Tada, Y. Shirota, and H. Mikawa, *Macromolecules*, **6**, 9 (1973).

7) Detailed results should be published soon.

8) a) K. Watanabe, T. Nakayama, and J. Mottl, *J. Quant. Spectrosc. Radiat. Transfer*, **2**, 369 (1962) ; b) D. W. Turner, C. Baker, A. D. Baker, and C. R. Brundle, "Molecular Photoelectron Spectroscopy," John Wiley and Sons, London (1970). The ionization potential (I) of MMA was assumed to be almost equal to that of methacrylaldehyde[8b] (I=9.8 eV). The ionization potential of VCZ was estimated to be about 7.9 eV from the energy of its charge-transfer band with CA [T. Nasuume, M. Nishimura, H. Fujimatsu, M. Shimizu, Y. Shirota, H. Hirata, S. Kusabayashi, and H. Mikawa, *Polymer J.*, **1**, 181 (1970)] by using the linear relation between the charge-transfer-band energies and the ionization potentials of the donors.[2b]

9) a) D. R. Kemp and G. Porter, *Chem. Commun.*, **1969**, 1029; b) D. R. Kemp and G. Porter, *Proc. R. Soc. London, Ser. A*, **326**, 117 (1971); c) G. Porter and M. R. Topp, *ibid.*, **315**, 163 (1970).

10) K. Kawai, Y. Shirota, H. Tsubomura, and H. Mikawa, *Bull. Chem. Soc. Jpn.*, **45**, 77 (1972).

11) a) S. K. Wong, L. Fabes, W. J. Green, and J. K. S. Wan, *J. Chem. Soc., Faraday Trans. 1*, **68**, 2211 (1972); b) S. K. Wong, W. Sytnyk, and J. K. S. Wan, *Can, J. Chem.*, **50**, 3052 (1972).

12) B. J. Hales and J. Bolton, *Photochem. Photobiol.*, **12**, 239 (1970).

13) A.-I. Kryukov and V. A. Krasnova, *Theor. Eksp. Khim.* **8**, 478 (1972); *Chem., Abstr.*, **78**, 130553d (1973).

14) a) H. Yoshida, Y. Kambara, and B. Rånby, *Bull. Chem. Soc. Jpn.*, **47**, 2599 (1974); b) Y. Kambara and H. Yoshida, Preprint for 34th Annual Meeting of Chemical Society of Japan, I, 282 (1976).

15) T. Natsuume, M. Nishimura, M. Fujimatsu, M. Shimizu, Y. Shirota, H. Hirata, S. Kusabayashi, and H. Mikawa, *Polymer J.*, **1**, 181 (1970).

16) a) N. Mataga, H. Kobashi, and T. Okada, *J. Phys. Chem.*, **73**, 370 (1969); b) H. Kobashi, T. Morita, and N. Mataga, *Chem. Phys. Lett.*, **20**, 376 (1973).

17) J. A. Riddick and W. B. Bunger, "Organic Solvents," in "Techniques of Chemistry," Vol. II, 3rd ed, ed by A. Weisberger, Wiley-Interscience, New York (1970).

18) J. Ulbricht, "Polymer Handbook," 2nd ed, ed by J. Brandrup and E. H. Immergut, Wiley-Interscience, New York (1975), p. 53.

19) For example, P. J. Flory, "Principles of Polymer Chemistry," Cornell University Press, New York (1953).

20) N. K. Bridge and G. Porter, *Proc. R. Soc. London, Ser A*, **244**, 276 (1958).

21) a) H. Masuhara, M. Shimada, and N. Mataga, *Bull. Chem. Soc. Jpn.*, **43**, 3316 (1970); b) H. Masuhara, M. Shimada, N. Tsujino, and N. Mataga, *ibid.*, **44**, 3310 (1971).

22) E. J. Land, *Trans Faraday Soc.*, **65**, 2815 (1969); R. Bensasson and E. J. Land, *ibid.*, **67**, 1904 (1971). We used the value of 7630 $\mathrm{mol^{-1}\,dm^3\,cm^{-1}}$ as the molar extinction coefficient, ε, of triplet benzophenone. In the latter article, the ε values of triplet duroquinone are given as 5330 and 6950 $\mathrm{mol^{-1}\,dm^3\,cm^{-1}}$ in cyclohexane and benzene respectively.

23) J. J. Andre and G. Weil, *Mol. Phys.*, **15**, 97 (1968).

24) In Fig. 9, when the straight line for the CAH· formation is extrapolated to the ionization potential of ST, it leads to an estimated value of $k_r \leq 10^8\ \mathrm{mol^{-1}\,dm^3\,s^{-1}}$ for the CA–ST system. Therefore, even if CAH· should be generated, its detection might be impossible because of the low yield, too low to register on our apparatus.

25) S. G. Cohen, A. Parola, and H. Parson, Jr., *Chem. Rev.*, **73**, 141 (1973).

26) S. Arimitsu, H. Masuhara, N. Mataga, and H. Tsubomura, *J. Phys. Chem.*, **79**, 1255 (1975).